

On the correction of conserved variables for numerical RMHD with staggered constrained transport

José-María Martí

*Departamento de Astronomía y Astrofísica
Universitat de València
E-46100 Burjassot (València)
SPAIN*

*Observatori Astronòmic
Universitat de València
E-46980 Paterna (València)
SPAIN*

Abstract

Despite the success of the combination of conservative schemes and staggered constrained transport algorithms in the last fifteen years, the accurate description of highly magnetized, relativistic flows with strong shocks represents still a challenge in numerical RMHD. The present paper focusses in the accuracy and robustness of several correction algorithms for the conserved variables, which has become a crucial ingredient in the numerical simulation of problems where the magnetic pressure dominates over the thermal pressure by more than two orders of magnitude.

Two versions of non-relativistic and fully relativistic corrections have been tested and compared using a magnetized cylindrical explosion with high magnetization ($\gtrsim 10^4$) as test. In the non-relativistic corrections, the total energy is corrected for the difference in the classical magnetic energy term between the average of the staggered fields and the conservative ones, before (CA1) and after (CA1') recovering the primitive variables. These corrections are unable to pass the test at any numerical resolution. The two relativistic approaches (CA2 and CA2'), correcting also the magnetic terms depending on the flow speed in both the momentum and the total energy, reveal as much more robust. These algorithms pass the test successfully and with very small

Email address: jose-maria.marti@uv.es (José-María Martí)

deviations of the energy conservation ($\lesssim 10^{-4}$), and very low values of the total momentum ($\lesssim 10^{-8}$). In particular, the algorithm CA2' (that corrects the conserved variables after recovering the primitive variables) passes the test at all resolutions.

The numerical code used to run all the test cases is briefly described.

Keywords: numerical RMHD, conservative schemes, constrained-transport schemes

1. Introduction

The popularization of the use of conservative methods in numerical RMHD, introduced in the late nineties (Koide et al., 1999; Komissarov, 1999a; Balsara, 2001), has revolutionized the research in several fields of Relativistic Astrophysics as, e.g., the study of the jets emanating from AGN (Komissarov, 1999b; Leismann et al., 2005; Keppens et al., 2008; Mignone et al., 2010; Mizuno et al., 2012), the structure and dynamics of pulsar wind nebulae (Komissarov & Lyubarsky, 2003; Del Zanna et al., 2004; Porth et al., 2013), or the production of GRB (Komissarov et al., 2009, 2010; Rezzolla et al., 2011).

To prevent the generation of artificial forces that can falsify the solutions, conservative schemes in numerical RMHD must be supplemented with some additional procedure to keep the magnetic field solenoidal along the simulation. Among the most successful strategies is the combination of numerical algorithms in conservation form to evolve cell-centered (finite-difference, finite-volume) representations of the hydrodynamical variables, and constrained transport (CT) algorithms for the magnetic field discretized on a staggered grid. The CT scheme, based in the conservation of magnetic flux across closed surfaces, maintains the value of the divergence of the magnetic field to the accuracy of machine round-off errors on a specific discretization. It was originally developed for artificial viscosity methods (Evans & Hawley, 1988). Dai & Woodward (1998), Ryu et al. (1998), and Balsara & Spicer (1999) combined the CT discretization with conservative schemes. Londrillo & Del Zanna (2000, 2004) developed the upwind constrained transport (UCT) strategy, which extends the CT method to high-order upwind schemes. At present, many RMHD codes (Komissarov, 1999a; Del Zanna et al., 2003; Leismann et al., 2005; Shibata & Sekiguchi, 2005; Antón et al., 2006; Mignone & Bodo, 2006; Mignone et al., 2007; Giacomazzo & Rezzolla, 2007; Del Zanna et al., 2007; Etienne et al., 2010; Beckwith & Stone, 2011)

use this approach.

The combination of conservative algorithms and staggered CT schemes has proven to be very succesful in the simulation of highly magnetized, relativistic flows with strong shocks. However the existence of two sets of variables defined on different grids requires in the most extreme cases some additional work to make the conservative and CT steps fully consistent. The proposed solutions (Komissarov, 1999a; Balsara & Spicer, 1999; Tóth, 2000; Mignone & Bodo, 2006) rely on correcting the conserved quantities after each time step to make them consistent with the staggered fields. The present paper explores the performance of several correction algorithms focussing in their accuracy and robustness.

The evolution system guarantees the fulfillment of this constraint for an initially divergence-free magnetic field at all later times, but to satisfy the constraint in numerical simulations of MHD flows poses a challenge.

2. Conservative methods for RMHD and Constrained Transport

2.1. The RMHD equations in conservation form

The equations of ideal RMHD, representing the conservation of rest-mass, momentum and energy of the magnetized fluid together with the induction equation can be written as a system of conservation laws¹. In Minkowski spacetime and Cartesian coordinates ($\{i, j, k\} = \{x, y, z\}$) this system reads²

$$\frac{\partial \mathbf{U}}{\partial t} + \frac{\partial \mathbf{F}^i(\mathbf{U})}{\partial x^i} = 0, \quad (1)$$

where the vector of conserved variables, \mathbf{U} , and the fluxes, \mathbf{F}^i , are the column vectors,

$$\mathbf{U} = \begin{pmatrix} D \\ S^j \\ E \\ B^k \end{pmatrix}, \quad (2)$$

¹The solenoidal condition for the magnetic field is guaranteed by the evolution system however it is by no means trivial to satisfy numerically.

²Throughout this paper, besides using units in which the speed of light is set to unity, a factor $\sqrt{4\pi}$ is absorbed in the definition of the magnetic field.

$$\mathbf{F}^i = \begin{pmatrix} Dv^i \\ S^j v^i + p^* \delta^{ij} - b^j B^i / W \\ Ev^i + p^* v^i - b^0 B^i / W \\ v^i B^k - v^k B^i \end{pmatrix}. \quad (3)$$

In these equations, D , S^j , E and B^k are the rest-mass density, the momentum density of the magnetized fluid in j -direction, the total energy density, and the magnetic field measured in the laboratory frame,

$$D = \rho W, \quad (4)$$

$$S^j = \rho h^* W^2 v^j - b^0 b^j, \quad (5)$$

$$E = \rho h^* W^2 - p^* - (b^0)^2, \quad (6)$$

where ρ is the proper rest-mass density of the fluid, p^* is the total pressure, and h^* is the specific enthalpy including the contribution of the magnetic field. These two last quantities are defined according to

$$p^* = p + \frac{b^2}{2} \quad (7)$$

$$h^* = 1 + \varepsilon + p/\rho + b^2/\rho, \quad (8)$$

where p is the fluid pressure and ε its specific internal energy. b^μ ($\mu = 0, 1, 2, 3$) are the components of the 4-vector representing the magnetic field in the fluid rest frame and b^2 stands for $b^\mu b_\mu$, where summation over repeated indices is assumed. v^i are the components of the fluid 3-velocity in the laboratory frame, which are related to the flow Lorentz factor, W , according to:

$$W = \frac{1}{\sqrt{1 - v^i v_i}}. \quad (9)$$

The following relations hold between the components of the magnetic field 4-vector in the comoving frame and the three vector components B^i measured in the laboratory frame:

$$b^0 = W \mathbf{B} \cdot \mathbf{v}, \quad (10)$$

$$b^i = \frac{B^i}{W} + b^0 v^i, \quad (11)$$

where \mathbf{v} and \mathbf{B} denote the 3-vectors (v^x, v^y, v^z) and (B^x, B^y, B^z) , respectively. The square of the modulus of the magnetic field can be written as

$$b^2 = \frac{B^2}{W^2} + (\mathbf{B} \cdot \mathbf{v})^2 \quad (12)$$

with $B^2 = B^i B_i$.

An equation of state that relates the thermodynamic variables, e.g., $p = p(\rho, \varepsilon)$, is needed to close the system.

To make more clear the corrections to be performed on them, the momentum and total energy densities are written making explicit their dependence on the magnetic field in the laboratory frame, \mathbf{B}

$$S^j = (\rho h W^2 + B^2) v^j - (\mathbf{v} \cdot \mathbf{B}) B^j, \quad (13)$$

$$E = \rho h W^2 - p + \frac{B^2}{2} + \frac{v^2 B^2 - (\mathbf{v} \cdot \mathbf{B})^2}{2} \quad (14)$$

($v^2 = v^i v_i$, $h = 1 + \varepsilon + p/\rho$).

2.2. Conservative methods for RMHD and Constrained Transport

Conservative methods exploit the conservation properties of the system of equations and can be directly applied to solve the equations of ideal RMHD written in conservation form, Eq. (1).

In these methods,

$$\frac{d\mathbf{U}_{i,j,k}}{dt} = \mathcal{L}_{i,j,k}^x + \mathcal{L}_{i,j,k}^y + \mathcal{L}_{i,j,k}^z, \quad (15)$$

where $\mathbf{U}_{i,j,k}$ is the value of the conserved variable \mathbf{U} at the point (x_i, y_j, z_k) (finite-difference approach) or its volume average at the cell centered in that point (finite-volume approach), and

$$\mathcal{L}_{i,j,k}^x = -\frac{1}{\Delta x_i} \left(\hat{\mathbf{F}}_{i+1/2,j,k}^x - \hat{\mathbf{F}}_{i-1/2,j,k}^x \right) \quad (16)$$

(and similar expressions for $\mathcal{L}_{i,j,k}^y$ and $\mathcal{L}_{i,j,k}^z$). Quantities $\hat{\mathbf{F}}_{i+1/2,j,k}^x$ are the numerical fluxes. In the Godunov-type methods (finite-volume approach), these fluxes are obtained from the solution of Riemann problems at cell interfaces $(x_{i+1/2}, y_j, z_k)$, where the initial left and right states, $\mathbf{U}_{L,i+1/2}$, $\mathbf{U}_{R,i+1/2}$ are reconstructed values from the corresponding cell averages.

The algorithm defined in Eq. (15) can be used to evolve system (1) in time. However, additional care has to be taken to prevent the divergence of the magnetic field to grow with time. Staggered CT algorithms maintain the divergence of \mathbf{B} exactly (i.e., to the accuracy of machine round-off errors) in each numerical cell. In this approach, the normal component of the surface-centered magnetic field on the cell interface at $(x_{i+1/2}, y_j, z_k)$ is evolved according to a discretized version of the induction equation

$$\begin{aligned} \frac{dB_{i+1/2,j,k}^x}{dt} = & \frac{1}{\Delta y} (\hat{\Omega}_{i+1/2,j+1/2,k}^z - \hat{\Omega}_{i+1/2,j-1/2,k}^z) - \\ & \frac{1}{\Delta z} (\hat{\Omega}_{i+1/2,j,k+1/2}^y - \hat{\Omega}_{i+1/2,j,k-1/2}^y), \end{aligned} \quad (17)$$

where quantities $\hat{\Omega}^i$ are discretized representations of the components of $\mathbf{\Omega} = \mathbf{v} \times \mathbf{B}$ computed at cell edges in terms of spatial and temporal interpolations of the magnetic field and the velocity, or the numerical fluxes of the conservative step.

Once the staggered magnetic fields have been computed, the corresponding cell-centered fields can be obtained by interpolation. For second order accuracy, a linear interpolation is enough and

$$B_{i,j,k}^x = \frac{1}{2} (B_{i-1/2,j,k}^x + B_{i+1/2,j,k}^x) \quad (18)$$

(and similar expressions for $B_{i,j,k}^y$ and $B_{i,j,k}^z$).

In its simplest version, the evolution scheme consists of a conservative step in which the rest-mass, momentum and energy densities are advanced in time, and a CT step to advance the staggered magnetic fields and obtain the cell-centered ones. Finally, inherent to all the conservative methods in RMHD is to solve an implicit algebraic system to recover the primitive variables (needed to compute the numerical fluxes), $\mathbf{V} = (\rho, p, v^i, B^k)$ from the conserved ones, \mathbf{U} , at every time step.

2.3. Setting the problem

According to the previous algorithm, at time $t = t^{n+1}$, the conserved variables have been advanced consistently with the magnetic fields defined at cell centers in the previous time step and are hence consistent with a magnetic field at cell centers, $B_{\text{cell},i,j,k}^{x,n+1}$, $B_{\text{cell},i,j,k}^{y,n+1}$ as computed with the cell-centered scheme (conservative step). However these fields are different from those

defined at cell centers, $B_{\text{stag},i,j,k}^{x,n+1}$, $B_{\text{stag},i,j,k}^{y,n+1}$ as the average of the staggered fields using Eq. (18). The fact that these two sets of magnetic fields are different is on the basis of the inconsistency of the algorithm, which makes it unsuitable for problems where the magnetic pressure dominates over the thermal pressure by more than two orders of magnitude.

The proposed solutions (Komissarov, 1999a; Balsara & Spicer, 1999; Tóth, 2000; Mignone & Bodo, 2006) rely on redefining the conserved quantities after each time step to make them consistent with the staggered field.

3. Correction of the conserved variables

Relying in the approach proposed by Balsara & Spicer (1999) for classical MHD, Mignone & Bodo (2006) proposed a non-relativistic correction of the conserved energy after each time step according to

$$E_{\text{stag}} = E_{\text{cell}} - \frac{B_{\text{cell}}^2 - B_{\text{stag}}^2}{2}. \quad (19)$$

In the previous expression, \mathbf{B}_{cell} and \mathbf{B}_{stag} are, respectively, the magnetic fields at some cell as computed in the conservative step, and by averaging the staggered fields. E_{cell} and E_{stag} are the corresponding conserved energy densities.

The procedure is computationally efficient since it does not involve extra calls to the primitive recovery procedure per time step, although as the rest of correction algorithms proposed, it forces to evolve the two equations of the magnetic field components normal to the sweep in the conservative step³. On the other hand, the non-relativistic nature of the correction dismisses all the magnetic terms depending on the flow velocity in the momentum and energy densities, making this correction questionable in those cases combining highly relativistic flow velocities and large magnetic fields.

This correction can be applied in two ways depending whether the correction of the energy is done before (correction algorithm CA1) or after (CA1')

³Since all the procedures are based on the advance in time of the cell-centered magnetic fields with the conservative algorithm, the number of three-dimensional variables increases in three. However, besides the additional calls to the primitive recovery procedure, where appropriate, the only extra computational cost is the pure advance of the two magnetic field components normal to the direction of the sweep, since these components are also reconstructed and used in the solution of the Riemann problems even in the case of no correction.

recovering the primitive variables. A potential drawback of the second approach is that hydrodynamic, primitive variables are not made consistent with the staggered fields.

In this work, we propose a full-relativistic correction in which the non-relativistic procedure CA1 is used as a first approximation. The correction (CA2) proceeds as follows:

1. Obtain an approximation to the total energy consistent with the staggered fields:

$$E_{\text{stag}}^{(1)} = E_{\text{cell}} - \frac{B_{\text{cell}}^2 - B_{\text{stag}}^2}{2}. \quad (20)$$

2. Obtain an approximation to the primitive variables, namely $\mathbf{V}^{(1)}$, from $\{D, \mathbf{S}, E_{\text{stag}}^{(1)}, \mathbf{B}_{\text{stag}}\}$.
3. Use the flow velocity $\mathbf{v}^{(1)}$ to complete the relativistic correction of the momentum and energy densities:

$$S_{\text{stag}}^{i(2)} = S^i - (B_{\text{cell}}^2 - B_{\text{stag}}^2)v^{i(1)} + \mathbf{v}^{(1)} \cdot (B_{\text{cell}}^i \mathbf{B}_{\text{cell}} - B_{\text{stag}}^i \mathbf{B}_{\text{stag}}) \quad (21)$$

$$E_{\text{stag}}^{(2)} = E_{\text{stag}}^{(1)} - \frac{(v^{(1)})^2}{2}(B_{\text{cell}}^2 - B_{\text{stag}}^2) + \frac{(\mathbf{v}^{(1)} \cdot \mathbf{B}_{\text{cell}})^2 - (\mathbf{v}^{(1)} \cdot \mathbf{B}_{\text{stag}})^2}{2} \quad (22)$$

4. Obtain the primitive variables from $\{D, \mathbf{S}_{\text{stag}}^{(2)}, E_{\text{stag}}^{(2)}, \mathbf{B}_{\text{stag}}\}$.

Steps 1. and 2. correspond to the classical correction CA1. Steps 3. and 4. complete the relativistic correction. The procedure involves one extra call to the recovery of primitive variables.

Finally, as in the correction algorithm CA1', the recovery of the primitive variables can be done prior to the correction of the conserved variables, leading to a very simple and computationally efficient algorithm (CA2'). In this case, the primitive variables are recovered using the cell-centered magnetic fields as advanced by the conservative algorithm, \mathbf{B}_{cell} , and then the conserved variables recalculated from these primitive variables and \mathbf{B}_{stag} . This is the approach followed by Komissarov (1999a). As in the case of correction CA1', a potential drawback of this approach is that hydrodynamic, primitive variables are not made consistent with the staggered fields (but, in contrast to CA1', the corrected conserved variables do include the relativistic corrections).

4. Numerical tests

4.1. The numerical code

The basic ingredients of the code used to test the correction procedure are the following:

- i) Cell reconstruction: second-order accurate values of the primitive variables \mathbf{V} at the left and right ends of the cells are obtained with linear functions and several limiters (MINMOD, VAN LEER, MC). MC and VAN LEER limiters can be degraded to MINMOD in case of strong shocks. No jump is allowed in the normal component of \mathbf{B} at a cell boundary and the corresponding staggered magnetic field is used.
- ii) Riemann solvers: intercell numerical fluxes are computed by means of HLL and HLLC (Mignone & Bodo, 2006) Riemann solvers. Accurate bounds of the maximum speeds of left and right propagating waves are obtained by solving the corresponding characteristic equation for the left and right states of each numerical interface.
- iii) Time advance: the multidimensional equations of RMHD are advanced in time in an unsplit manner using TVD-preserving Runge-Kutta methods of second and third order (Shu & Osher, 1988, 1989). The time step is determined according to $\Delta t = \frac{CFL}{\sqrt{2}} \times \min_{i,j} \left(\frac{\Delta x}{|\lambda_{x,i,j}|}, \frac{\Delta y}{|\lambda_{y,i,j}|} \right)$ (2D, planar symmetry version), where $\lambda_{x,i,j}$ and $\lambda_{y,i,j}$ are the speeds of the fastest waves propagating in cell i, j along the x and y direction, respectively.
- iv) Constrained transport scheme as in Balsara & Spicer (1999).
- v) Primitive variables are recovered as in the $1D_W$ method of Noble et al. (2006) and solving the resulting equation in $Z = \rho h W^2$ by bisection.

The code advances the total energy density without the rest-mass energy density, i.e., $E - D$. This strategy improves the performance of the conservative scheme when the total energy is dominated by the rest-mass energy. However, in this case it does not produce any effect, since in the selected test (see next Section) the total energy density is larger than the rest-mass energy density by several orders of magnitude.

4.2. The test: cylindrical magnetized blast wave

The setup for this test is taken from Komissarov (1999a). A cylindrical region of radius $r = 0.8$ with density $\rho = 10^{-2}$ and thermal pressure $p = 1$ is embedded in a static uniform medium with $\rho = 10^{-4}$ and $p = 3 \times 10^{-5}$. A linear smoothing function is applied for $0.8 < r < 1$. The whole region is threaded by a constant horizontal magnetic field in the x -direction, $B_x = 1$. An ideal gas equation of state with $\gamma = 4/3$ is used.

The difference in pressure between the cylindrical region and the ambient medium produces the expansion of the central region delimited by a fast forward shock propagating radially at almost the speed of light. Because of the strong sideways magnetic confinement an elongated structure develops in the x direction with a maximum Lorentz factor of $W \simeq 4.5$. This problem is particularly challenging because of the very large magnetization $\beta = b^2/(2p) = 1.67 \times 10^4$.

The test is solved in Cartesian (x, y) coordinates. The numerical grid covers a $[-6, 6] \times [-6, 6]$ square with the center of the cylindrical region at $(0, 0)$. Open boundary conditions are placed along the boundaries of the computational domain.

A reference model using the HLLC Riemann solver and the third order Runge-Kutta (RK3) for time advance has been ran. For the cell reconstruction we have used the VAN LEER limiter degraded to MINMOD (VLMM) when the relative jump in thermal or magnetic pressure within a shock exceeds 0.5. The relativistic correction proposed in this paper (CA2) was chosen to correct the conserved variables after each time substep. A CFL of 0.45 and a numerical resolution of $N_x \times N_y = 512^2$ cells complete the initial setup. Figure 1 shows the distributions of proper rest-mass density, gas pressure and magnetic pressure (in logarithmic scale), and flow Lorentz factor at $t = 4.0$ as computed in the reference run. The fast magnetosonic shock and the elongated horizontal structure are clearly seen.

Table 1 displays the total momentum and the relative change in total energy at $t = 4.0$ for the different correction algorithms and several numerical resolutions from 128^2 to 1024^2 cells. For the reference model (CA2, $N_x \times N_y = 512^2$), the relative change in total energy is 2.60×10^{-5} , whereas the total momentum (initially equal to zero) reaches a value of 4.11×10^{-11} . The same run without energy nor momentum corrections (CA0) crashes at the sixth iteration ($t \simeq 0.03$), whereas the run using the classical correction (CA1) crashes at $t \simeq 0.39$. The same run using Komissarov (1999a)'s recipe (CA2'), completes the test normally and with a relative change in total energy

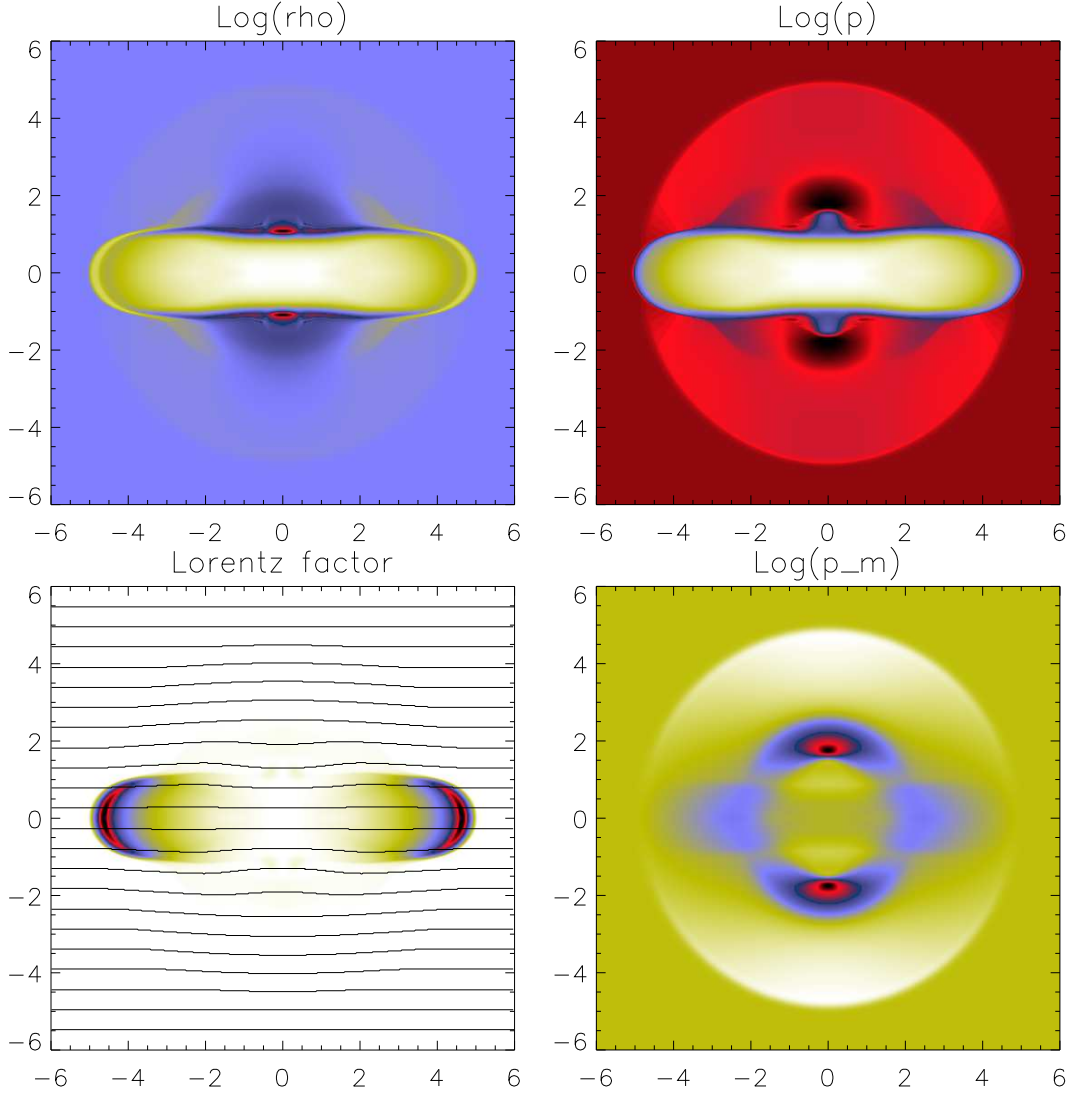


Figure 1: Proper rest-mass density, gas pressure and magnetic pressure (in logarithmic scale), and flow Lorentz factor at $t = 4.0$ as computed in the reference run of the cylindrical magnetized blast wave test discussed in the text. The magnetic field lines are printed on top of the Lorentz factor plot. $\log \rho \in [-5.30, -2.71]$, $\log p \in [-4.65, -0.94]$, $\log p_m \in [-0.60, -0.20]$, $W \in [1.00, 4.63]$.

Table 1: Total momentum (first row in two-row table entries) and relative change in total energy (secod row) in the cylindrical magnetized blast wave test discussed in the text at $t = 4.0$, as a function of the correction algorithm and numerical resolution. Table entries with a single number display the time at which the run stopped abnormally.

$N_x \times N_y$	CA0	CA1	CA1'	CA2	CA2'
128 ²	2.66×10^{-2}	1.13	1.18	1.19×10^{-11}	8.00×10^{-12}
				1.51×10^{-4}	1.55×10^{-4}
256 ²	2.29×10^{-2}	0.70	0.73	2.17×10^{-11}	7.50×10^{-10}
				7.69×10^{-5}	7.91×10^{-5}
512 ²	2.72×10^{-2}	0.39	0.42	4.11×10^{-11}	1.55×10^{-8}
				2.60×10^{-5}	2.70×10^{-5}
1024 ²	3.75×10^{-2}	0.31	0.37	3.43	7.94×10^{-9}
					8.08×10^{-6}

of 2.70×10^{-5} and a total momentum of 1.55×10^{-8} . The parameters chosen (VLMM,HLLC,RK3) produce a version of the code with very low dissipation, which makes the algorithms without correction algorithm (CA0) and with the classical correction (CA1) to fail in passing the test at any resolution. Code versions using corrections CA2 and CA2' pass the test succesfully and with very small deviations of the energy conservation ($\lesssim 10^{-4}$), and very low values of the total momentum ($\lesssim 10^{-8}$). In the case of the relativistic correction CA2, the run stopped abnormally for the largest resolution (1024²) close to the end of the test, at $t = 3.43$.

In flows with high magnetization, accuracy problems can lead to unphysical internal energies and pressures. The correction algorithm CA2' can be affected by this failure since in this case the recovery of primitive variables is done before the correction of the conserved variables and are then obtained from cell-centered representations of the magnetic field as advanced in the conservative step. In Table 2, the maximum and average relative differences in thermal pressure at $t = 4.0$ for the cases using the correction algorithms CA2 and CA2' and numerical resolutions $N_x \times N_y = 128^2, 256^2, 512^2$, are shown. The values of the average relative pressure difference between both algorithms tend to zero with numerical resolution, whereas the maximum rel-

Table 2: Maximum and average relative differences in thermal pressure for the cases using correction algorithm CA2 and CA2', in the cylindrical magnetized blast wave test discussed in the text at $t = 4.0$. The maximum relative difference is computed as $\max_{i,j} \left\{ \frac{|p_{CA2}(i,j) - p_{CA2'}(i,j)|}{p_{CA2}(i,j)} \right\}$. The average relative difference is computed as $\frac{\sum_{i,j} |p_{CA2}(i,j) - p_{CA2'}(i,j)|}{\sum_{i,j} p_{CA2}(i,j)}$. In these expressions, i, j span the whole numerical grid.

$N_x \times N_y$	max	aver
128^2	1.32×10^{-2}	5.53×10^{-5}
256^2	2.77×10^{-2}	2.75×10^{-5}
512^2	3.65×10^{-2}	8.65×10^{-6}

ative difference seems to increase with numerical resolution although keeping small values ($\approx 1 - 3\%$). The conclusion is that the pressure values obtained with the algorithm CA2' are consistent with those obtained with the algorithm CA2, in which the primitive variables are recovered once the conserved variables have been corrected.

The same test with $B_x = 10, 100$ (magnetizations $1.67 \times 10^6, 1.67 \times 10^8$, respectively) has been run without problems with the same algorithm choice (VLMM, HLLC, RK3) and correction algorithms CA2 and CA2' with a spatial resolution of 512^2 cells (see Fig. 2).

5. Summary and conclusions

Despite the success of the combination of conservative schemes and staggered constrained transport algorithms in the last fifteen years, the accurate description of highly magnetized, relativistic flows with strong shocks flows represents still a challenge in numerical RMHD. The present paper focusses in the accuracy and robustness of several correction algorithms for the conserved variables, which has become a crucial ingredient in the numerical simulation of problems where the magnetic pressure dominates over the thermal pressure by more than two orders of magnitude.

Two versions of non-relativistic and fully relativistic corrections have been tested and compared using a magnetized cylindrical explosion with high mag-

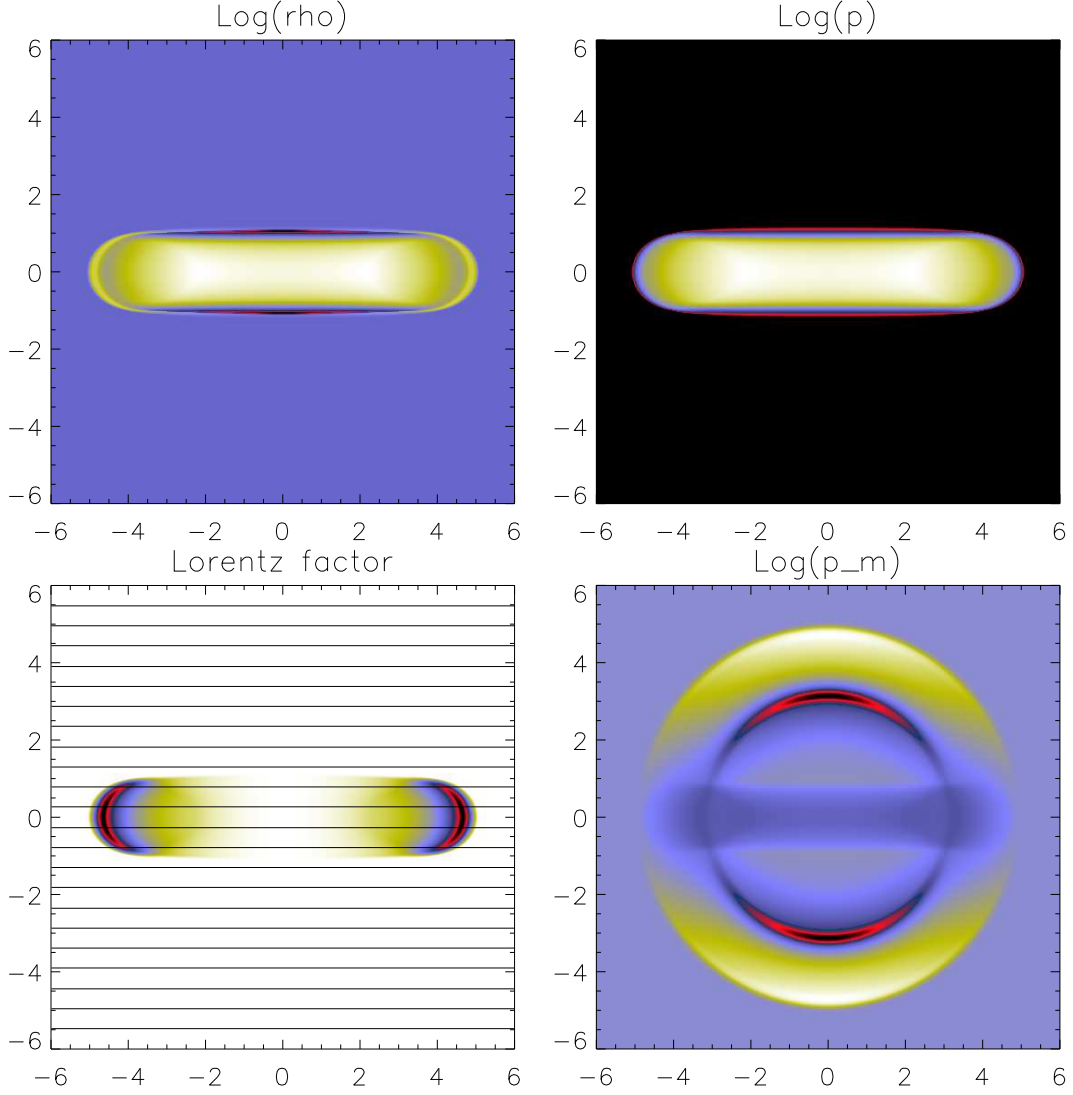


Figure 2: Proper rest-mass density, gas pressure and magnetic pressure (in logarithmic scale), and flow Lorentz factor at $t = 4.0$ as computed in the cylindrical magnetized blast wave test with $B_x = 100$ (magnetization 1.67×10^8) using the same algorithm choice as in the test run (VLMM,HLLC,RK3), correction algorithm CA2 and a spatial resolution of 512^2 cells. The magnetic field lines are printed on top of the Lorentz factor plot. $\log \rho \in [-4.83, -2.75]$, $\log p \in [-4.52, -1.00]$, $\log p_m \in [3.698950, 3.698986]$, $W \in [1.00, 4.68]$.

netization ($\gtrsim 10^4$) as test. In the non-relativistic corrections, the total energy is corrected for the difference in the classical magnetic energy term between the average of the staggered fields and the conservative ones, before (CA1) and after (CA1') recovering the primitive variables. These corrections are unable to pass the test at any numerical resolution. The two relativistic approaches (CA2 and CA2'), correcting also the magnetic terms depending on the flow speed in both the momentum and the total energy, reveal as much more robust. These algorithms pass the test successfully and with very small deviations of the energy conservation ($\lesssim 10^{-4}$), and very low values of the total momentum ($\lesssim 10^{-8}$). In particular, the algorithm CA2' (that corrects the conserved variables after recovering the primitive variables) passes the test at all resolutions.

The numerical code used to run all the test cases is briefly described.

Acknowledgements. J.-M. M. acknowledges financial support from the Spanish Ministerio de Economía y Competitividad (grants AYA2013-40979-P, and AYA2013-48226-C3-2-P). The author also acknowledges the referee, L. Del Zanna, for his comments, which have contributed to improve the first version of the manuscript.

Antón, L., Zanotti, O., Miralles, J. A., Martí, J. M., Ibáñez, J. M., Font, J. A. & Pons, J. A. (2006), *ApJ*, **637**, 296

Balsara, D.S. (2001), *ApJS*, **132**, 83

Balsara, D.S. & Spicer, S.D. (1999), *JCP*, **149**, 270

Beckwith, K. & Stone, J. M. (2011), *ApJS*, **193**, article id. 6

Dai, W. & Woodward, P. R. (1998), *ApJ*, **494**, 317

Del Zanna, L., Bucciantini, N. & Londrillo, P. (2003), *A&A*, **400**, 397

Del Zanna, L., Amato, E. & Bucciantini, N. (2004), *A&A*, **421**, 1063

Del Zanna, L., Zanotti, O., Bucciantini, N. & Londrillo, P. (2007), *A&A*, **473**, 11

Etienne, Z. B., Liu, Y. T. & Shapiro, S. L. (2010), *PRD*, **82**, id. 084031

Evans, C. R. & Hawley, J. F. (1988), *ApJ*, **332**, 659

- Giacomazzo, B. & Rezzolla, L. (2007), CQG, **24**, S235-S258
- Keppens, R., Meliani, Z., van der Holst, B. & Casse, F. (2008), A&A, **486**, 663
- Koide, S., Shibata, K. & Kudoh, T. (1999), ApJ, **522**, 727
- Komissarov, S.S. (1999a), MNRAS, **303**, 343
- Komissarov, S.S. (1999b), MNRAS, **308**, 1069
- Komissarov, S. S.& Lyubarsky, Y. E. (2003), MNRAS, **344**, L93
- Komissarov, S. S., Vlahakis, N. & Königl, A. (2010), MNRAS, **407**, 17
- Komissarov, S. S., Vlahakis, N., Königl, A. & Barkov, M.V. (2009), MNRAS, **394**, 1182
- Leismann, T., Antón, L., Aloy, M. A., Müller, E., Martí, J. M., Miralles, J. A. & Ibáñez, J. M. (2005), A&A, **436**, 503
- Londrillo, P. & Del Zanna (2000), ApJ, **530**, 508
- Londrillo, P. & Del Zanna (2004), JCP, **195**, 17
- Mignone, A. & Bodo G. (2006), MNRAS, **368**, 1040
- Mignone, A., Bodo, G., Massaglia, S., Matsakos, T., Tesileanu, O., Zanni, C. & Ferrari, A. (2007), ApJS, **170**, 228
- Mignone, A., Rossi, P., Bodo, G., Ferrari, A. & Massaglia, S. (2010), MNRAS, **402**, 7
- Mizuno, Y., Lyubarsky, Y., Nishikawa, K.-I. & Hardee, P. E. (2012), ApJ, **757**, article id. 16
- Noble, S.C., Gammie, C.F., McKinney, J.C. & Del Zanna, L. (2006), ApJ, **641**, 626
- Porth, O., Komissarov, S. S. & Keppens, R. (2013), MNRAS, **431**, L48
- Rezzolla, L., Giacomazzo, B., Baiotti, L., Granot, J., Kouveliotou, C. & Aloy, M. A. (2011), ApJL, **732**, article id. L6

- Ryu, D., Miniati, F., Jones, T. W. & Frank, A. (1998), ApJ, **509**, 244
- Shibata, M. & Sekiguchi, Y.-I. (2005), PRD, **72**, id. 044014
- Shu, C.W. & Osher, S.J. (1988), JCP, **77**, 439
- Shu, C.W. & Osher, S.J. (1989), JCP, **83**, 32
- Tóth, G. (2000), JCP, **161**, 605